

NEXT-GENERATION ALL-SOLID-STATE BATTERY (#ASSB)

Tuan Vo^{a,b,†}, Claas Hüter^b, Stefanie Braun^a, Manuel Torrilhon^a

^aDepartment of Mathematics, Applied and Computational Mathematics (ACoM), RWTH Aachen University, Schinkelstraße 02, 52062 Aachen, Germany

^bInstitute of Energy and Climate Research (IEK-2), Forschungszentrum Jülich, Wilhelm-Johnen-Straße, 52428 Jülich, Germany

Mathematical modelling for the next-generation All-solid-state batteries: Nucleation (SE|SSE)^(*)-interface

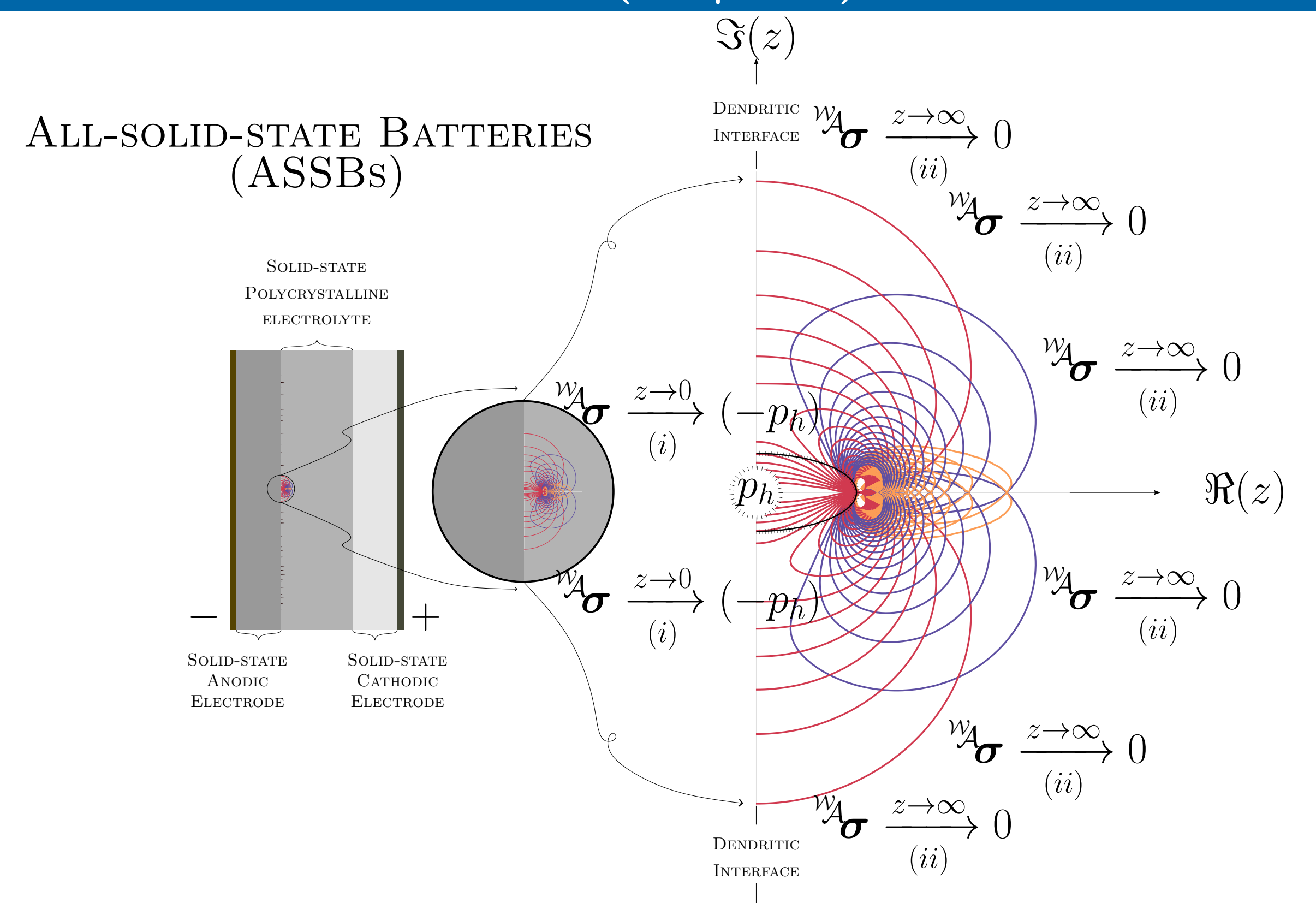
Rechargeable Lithium-ion battery (LIB) is at the heart of every electric vehicle (EV), portable electronic device, and energy storage system [1]. Nowadays, LIBs enable human life more efficient and help to solve global environment issues thanks to EVs' zero emission. However, conventional LIB (c-LIB) is sensible to temperature and pressure, hence, flammable and explosive, which is undesirable. This bottleneck is mainly due to **liquid-based electrolyte** found in c-LIBs.

All-solid-state battery (ASSB) is one of promising candidates to overcome bottlenecks of c-LIBs. Thanks to **solid-state electrolyte** (SSE), ASSB is highly stable towards temperature and pressure. Nevertheless, Li-metal dendrite triggered at (SE|SSE)-interface is the main drawback of ASSB since these dendritic threads extrapolate into SSE grain boundary network, causing crevice, degradation of ionic conductivity, and the probability of short-circuit, which is unfavorable.

Next-generation All-solid-state battery (ng-ASSB) with a consideration of **nucleation criterion** defined by

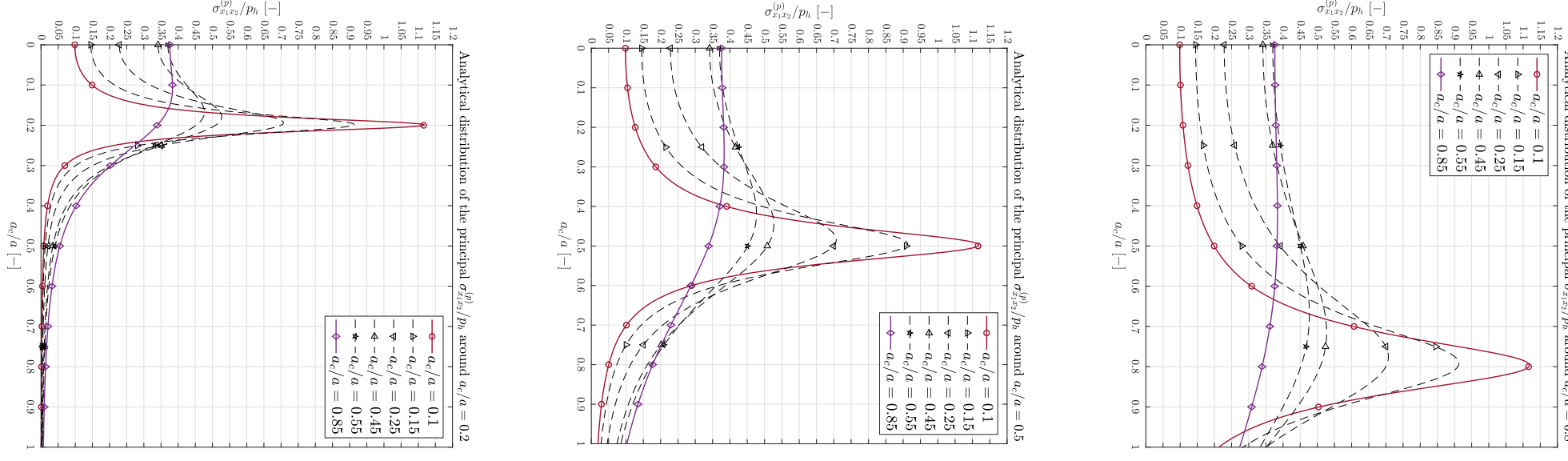
$$a_{\text{Griffith}} := a^* = \arg \min_{a \in \mathbb{R}} \iint_{\Omega} f(a, \mathbf{u}, \theta; \lambda, \mu, \mathbf{d} \otimes \mathbf{d}) d\Omega - \iint_{\Gamma} f(a; \gamma) d\Gamma \Big|_{\mathbf{u}^{(s)}}$$

where \mathbf{u} displacement field, θ temperature field, a crevice length, λ, μ Lamé constants, $\mathbf{d} \otimes \mathbf{d}$ embedded misorientation structural tensor, and γ cracking-surface energy density, can help to improve ASSB performance.



Interface Analysis

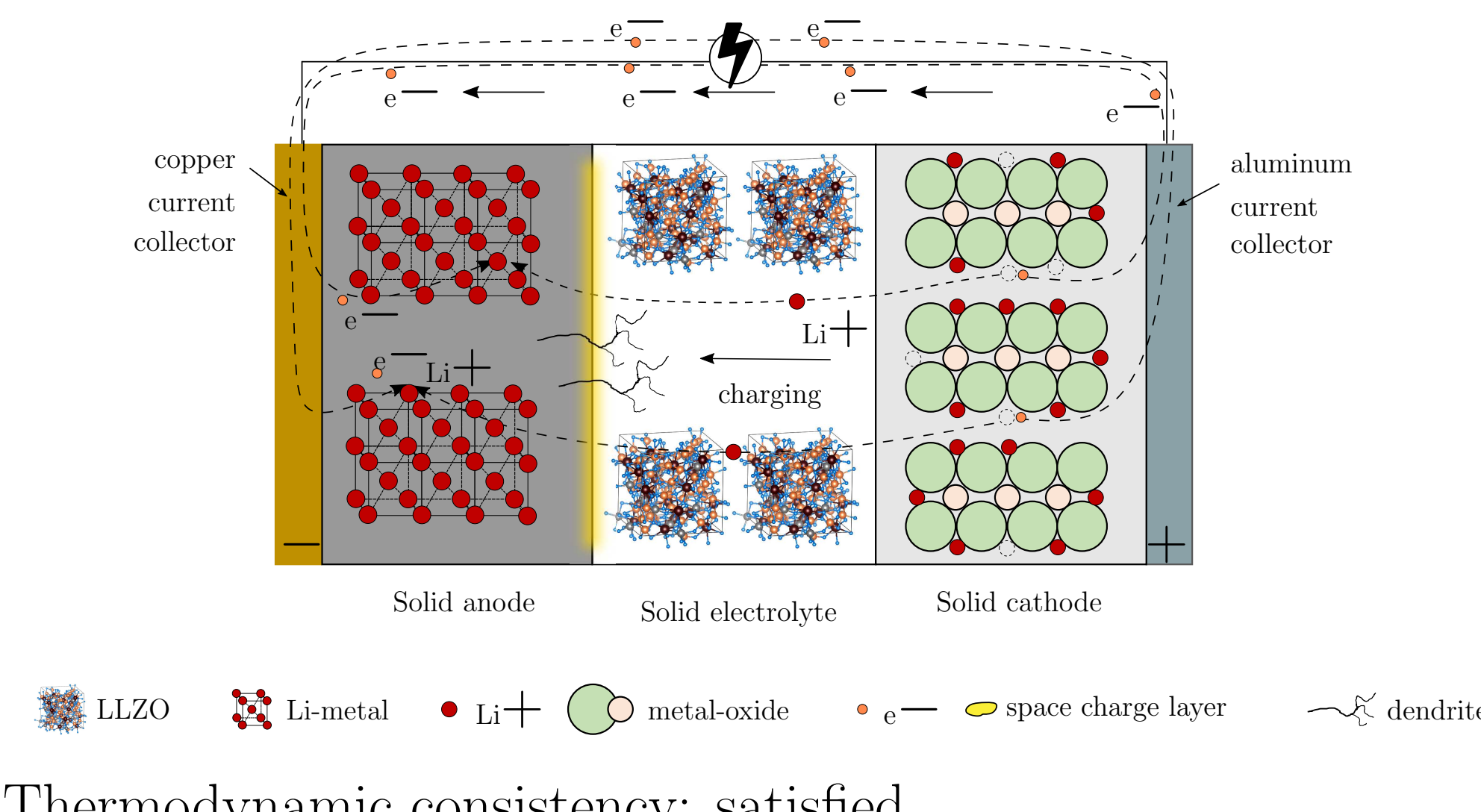
Interface between solid electrode and solid-state electrolyte (SE|SSE) taking place at space charge layer (SCL) [2] found in ASSBs critically exhibits mechanical and electrochemical instability [3]. This evidence points directly to the fact that the soft metallic li anode is erroneously prone to triggering dendrites, under cycles of electric charge & discharge [4].



Distribution: ana. max. shear stress $w_A \sigma_{\pi}$ around crack tip a_c .

Next-generation All-solid-state battery

Nucleation taking place at critical dendritic (SE|SSE)-interface

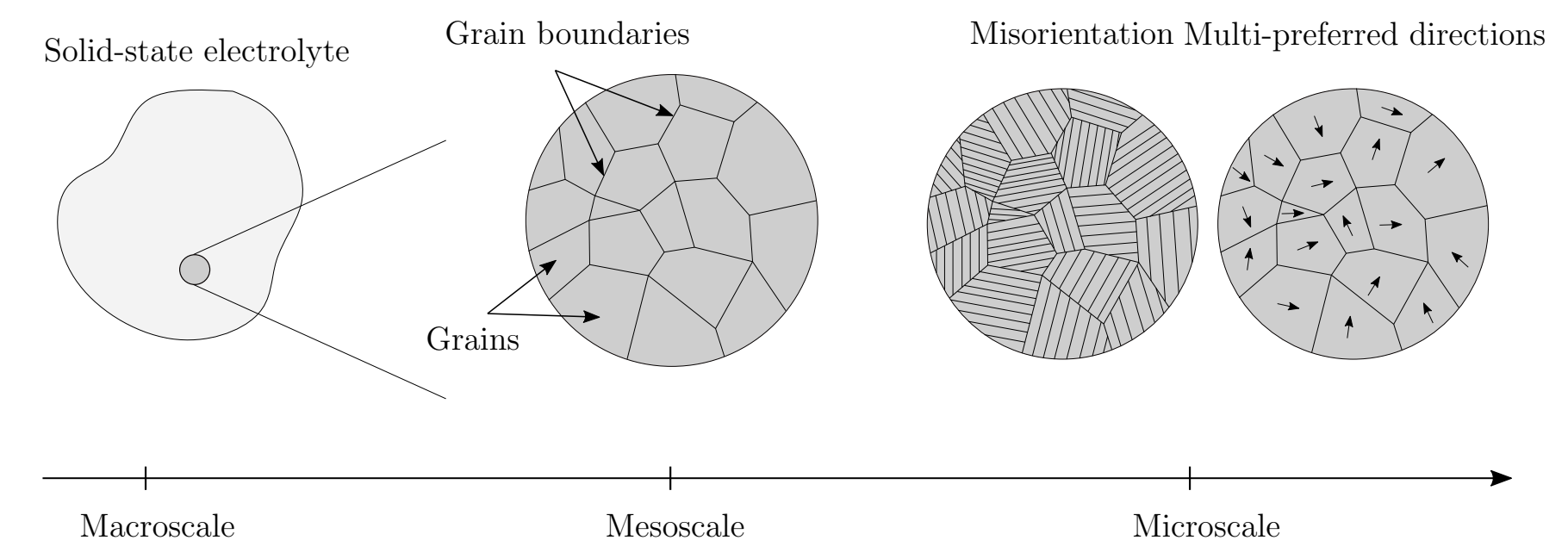


Thermodynamic consistency: satisfied.

Closure problem: fulfill by 15 moments.

Embedded structural-tensor SSE

Polycrystalline garnet-typed SSE such as LLZO exhibit a network of grain boundaries, and grains with various sizes and shapes under microscopic observation. Therefore, this type of microstructure is potentially prone to nuance destruction of ceramic-like materials.



Consequently, dendrites contribute to degradation of ionic conductivity and cracks via tracing along grain boundaries.

Nucleation interface: Taking place at the critical dendritic interface

Coupled fields: Displacement vector field and temperature scalar field

$$\mathbf{u} : \begin{cases} \Omega \times \mathbb{R}_+ \rightarrow \mathbb{R}^3, \\ (\mathbf{x}, t) \mapsto \mathbf{u}(\mathbf{x}, t), \end{cases} \quad \theta : \begin{cases} \Omega \times \mathbb{R}_+ \rightarrow \mathbb{R}, \\ (\mathbf{x}, t) \mapsto \theta(\mathbf{x}, t), \end{cases} \quad \theta : \begin{cases} \Omega \times \mathbb{R}_+ \rightarrow \mathbb{R}, \\ (\mathbf{x}, t) \mapsto \theta(\mathbf{x}, t), \end{cases}$$

Governing conservation equations

$$\frac{d}{dt} \int_{\Omega} (\cdot) d\Omega = \int_{\Omega} (\cdot)^{\text{action}} d\Omega + \int_{\partial\Omega} (\cdot)^{\text{action}} d\partial\Omega + \int_{\Omega} (\cdot)^{\text{production/source/sink}} d\Omega$$

$\rho(\mathbf{x}, t)$ is mass density per unit volume (puv); $\mathbf{b}(\mathbf{x}, t)$ body force puv; $\mathbf{v}(\mathbf{x}, t)$ velocity; $e(\mathbf{x}, t)$ internal energy puv; $\mathbf{q}(\mathbf{x}, t)$ heat flux; $r(\mathbf{x}, t)$ heat source puv; $\boldsymbol{\sigma}$ Cauchy stress and $\boldsymbol{\varepsilon}$ infinitesimal strain. Helmholtz energy functional

$$a_{\text{Griffith}} := a^* = \arg \min_{a \in \mathbb{R}} \iint_{\Omega} f(a, \mathbf{u}; \lambda, \mu, \mathbf{d} \otimes \mathbf{d}) d\Omega - \iint_{\Gamma} f(a; \gamma) d\Gamma \Big|_{\mathbf{u}^{(s)}}$$

Governing PDE

$$a_{\text{Griffith}} := a^* = \arg \min_{a \in \mathbb{R}} \iint_{\Omega} f(a, \mathbf{u}; \lambda, \mu, \mathbf{d} \otimes \mathbf{d}) d\Omega - \iint_{\Gamma} f(a; \gamma) d\Gamma \Big|_{\mathbf{u}^{(s)}}$$

abc

Strain energy: Interface between solid electrode and solid-state electrolyte (SE|SSE) taking place at space charge

$$\iint_{\Omega} f(a, \mathbf{u}; \lambda, \mu, \mathbf{d} \otimes \mathbf{d}) d\Omega$$

Surface energy: Interface between solid electrode and solid-state electrolyte (SE|SSE) taking place

$$\iint_{\Gamma} f(a; \gamma) d\Gamma$$

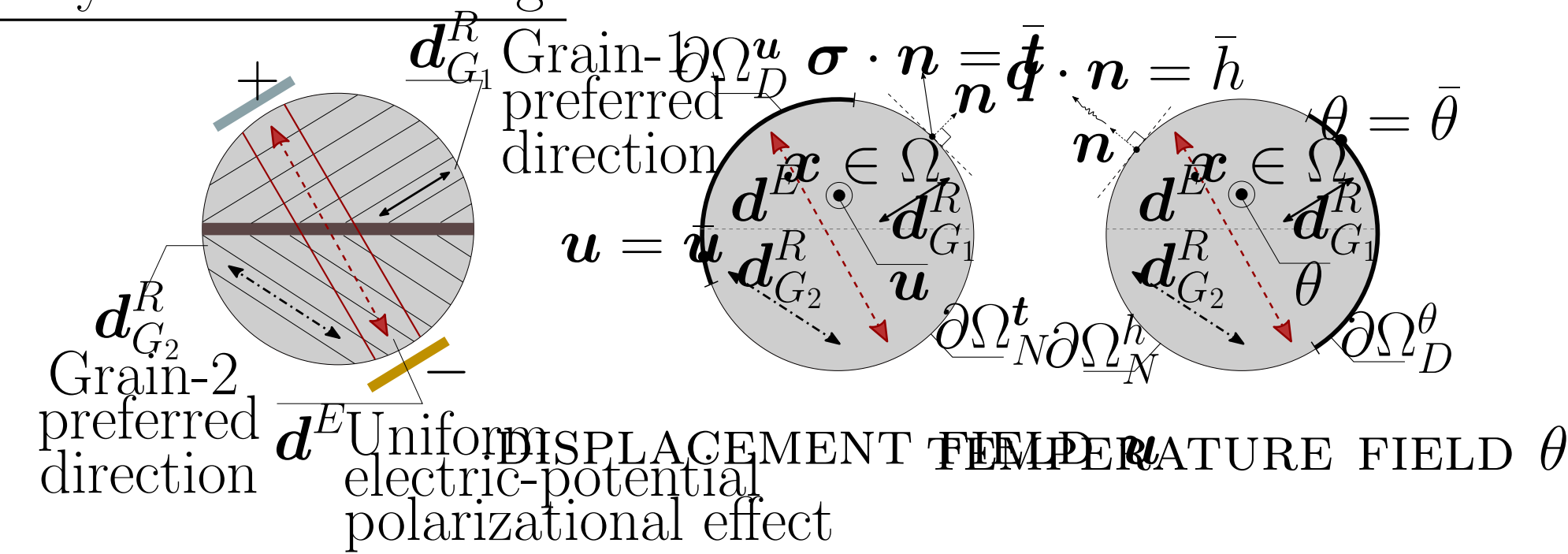
Therefore

$$\rho \partial_t^2 \mathbf{u}^{(s)} + \nabla \cdot \left(\mathbb{C}^{J(\lambda, \mu)} : \nabla \mathbf{u}^{(s)} \right) + \rho \nabla V_e = \mathbf{0},$$

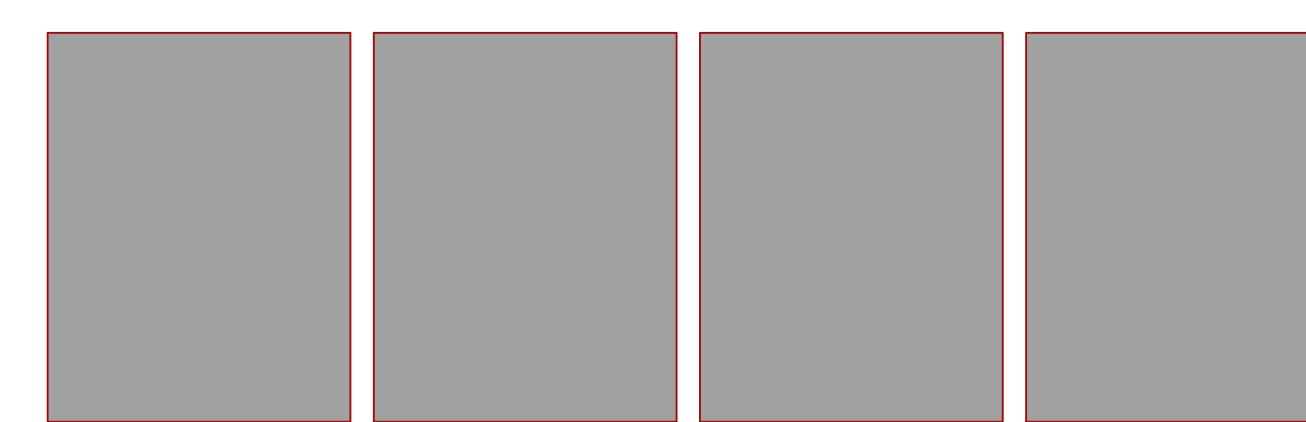
$$\text{s.t. } a_{\text{Griffith}} := a^* = \arg \min_{a \in \mathbb{R}} \iint_{\Omega} f(a, \mathbf{u}; \lambda, \mu, \mathbf{d} \otimes \mathbf{d}) d\Omega - \iint_{\Gamma} f(a; \gamma) d\Gamma \Big|_{\mathbf{u}^{(s)}}$$

abc

Boundary condition settings



Comparison: Analytical vs. Numerical solutions



Airy-Westergaard function used for max. shear stress analysis

$$w_A : \mathbb{C} \rightarrow \mathbb{C}, z \mapsto w_A(z) := \Re \left(\oint_{\Gamma} \mathcal{K}^{(*)} dz \right) + x_2 \Im \left(\oint_{\Gamma} \mathcal{K}^{(*)} dz \right), \mathcal{K}^c(z) := -p_h + p_h / \sqrt{1 - a^2/z^2},$$

where $\{p_h, a\} \in \mathbb{R}_+$ is the.

FEM implementation: element matrix \mathbf{K}^e approx. by *Gauss quadrature*; indices imply 4+2 = 6 for-loop:

$$K_{ik}^{e\alpha\beta} = \int_{\Omega^e} \left(\mathcal{L}_1^{\alpha} \mathbb{C}_{ikl}^{fGL}(y) \mathcal{R}_1^{\beta} + \mathcal{L}_1^{\alpha} \mathbb{C}_{ikl}^{fGL}(y) \mathcal{R}_2^{\beta} + \mathcal{L}_2^{\alpha} \mathbb{C}_{ikl}^{fGL}(y) \mathcal{R}_1^{\beta} + \mathcal{L}_2^{\alpha} \mathbb{C}_{ikl}^{fGL}(y) \mathcal{R}_2^{\beta} \right) \det(\mathbf{J}) d\Omega^e$$

where \mathcal{L}_j^{α} and \mathcal{R}_l^{β} are gradients of basis functions at node α^{th} and β^{th} , respectively.

Contact

Tuan Vo
vo@acom.rwth-aachen.de



Scan me

References

- [1] **T.Vo**, *Modeling the swelling phenomena of li-ion batt. cells based on a numerical chemo-mech. coupled approach*. MA, Robert Bosch Battery Systems GmbH, 2018.
- [2] **S.Braun**, C.Yada and A.Latz, *Thermodynamically consistent model for Space-Charge-Layer formation in a solid electrolyte*. Jr. Phys. Chem., 119, 22281-22288, 2015.
- [3] **C.Hüter**, S.Fu, M.Finsterbusch, E.Figgemeier, L.Wells, and R.Spatschek, *Electrode-electrolyte interface stability in solid state electrolyte system: influence of coating thickness under varying residual stresses*. AIMS Materials Science, 4(4):867-877, 2017.
- [4] **S.Kim**, J.S.Kim, L.Miara, Y.Wang, S.K.Jung, S.Y.Park, Z.Song, H.King, M.Badding, J.M.Chang, V.Roev, G.Yoon, R.Kim, J.H.Kim, K.Yoon, D.Im, and K.Kang, *High-energy and durable li metal batt. using garnet-type solid electrolytes with tailored li-metal compatibility*. Nature Communications, 13(1):1883, 2022.